

We are IntechOpen, the world's leading publisher of Open Access books Built by scientists, for scientists

6,900

Open access books available

186,000

International authors and editors

200M

Downloads

Our authors are among the

154

Countries delivered to

TOP 1%

most cited scientists

12.2%

Contributors from top 500 universities



WEB OF SCIENCE™

Selection of our books indexed in the Book Citation Index
in Web of Science™ Core Collection (BKCI)

Interested in publishing with us?
Contact book.department@intechopen.com

Numbers displayed above are based on latest data collected.
For more information visit www.intechopen.com



Uranium Dioxide Nanoparticulated Materials

*Analía Leticia Soldati, Diana Carolina Lago
and Miguel Oscar Prado*

Abstract

Nanostructured actinide materials have gained the attention of the nuclear community after the discovery of enhanced properties in fuels that undergo high burn up. On these conditions, the UO_2 grains experimented recrystallization and formed a new rim of UO_2 nanoparticles, called high burn up structures (HBS). The pellets with HBS showed closed porosity with better fission gas retention and radiation tolerance, ameliorated mechanical properties, and less detriment of the thermal conductivity upon use. In this chapter, we will review different ways to obtain uranium nanoparticles, with emphasis on their synthesis and characterization. On the one hand, we will comment on radiation chemical syntheses, organic precursor-assisted syntheses, denitration processes, and biologically mediated syntheses. On the other hand, we will include for each of them a reference to the appropriate tools of the materials science that are used to fully characterize physical and chemical properties of these actinide nanoparticles.

Keywords: UO_2 , nanoparticles, grain sizes, synthesis, characterization

1. Introduction

Nanomaterials, which are present naturally in the environment and also as a result of anthropogenic activities (incidental or engineered), gain the attention of scientist and technologists due to their promising applications. The surface-to-volume ratio, grain size, morphology, composition and elemental distribution affect nanoparticle's physicochemical and electrical properties, surface reactivity, material growth, or dissolution rates [1]. These characteristics can be thus engineered to take advantage of the nanoparticles over their macroscopic equivalents, for example, to favor faster catalysis of reactions, high loading of medicines or absorption of toxins from polluted zones.

In the nuclear material's field, actinide oxides nanoparticles became under systematic study after the detection of two main issues:

First, the discovery of a rim structure in UO_2 pellets that had have a burn up of 40–67 GWd/tM (also called high burn up structures or HBS [2]). The pellet, initially formed by micrometer-sized grains recrystallized in a ring of nanoparticles at the rim. The pellets with HBS presented better fission gas retention, ameliorated radiation tolerance and mechanical properties as the plasticity [3]. The direct consequence of this observation was an increment in the number of publications dealing with different synthesis of UO_2 nanoparticles to form pellets mimicking from the beginning the HBS structure [3–7].

Second, the fact that actinides tend to form colloids of aggregated nanoparticles [8, 9]. Indeed, in contact with water, metallic U corrosion is known to form fine UO_2 particulates [10, 11]. This material has different properties than micrometer particulated material, affecting, for example, the expected behavior in spent nuclear fuels, radioactive wastes, and contaminated places, due to their differences in mobility, solubility, surface reactivity, complexation, speciation, weathering, eco-toxicity, and biological uptake. In particular, because their small size, nanoparticles may have a toxic effect on living organisms that is not present with micrometer-sized particles. Thus, there is a need for expanding the actual knowledge on actinide nanoparticles with emphasis in their physicochemical properties, grain sizes, crystal phases, elemental distribution and reactivity, for predicting and controlling their behavior under different conditions. This knowledge will also serve to redesigning long-term nuclear waste disposals and mobility barriers.

Both former topics request well-characterized actinide nanoparticles, especially those composed of UO_2 . That, added to the scientific motivation per se, is represented in the increased number of publications in the past 25 years dealing with different synthesis and characterization of UO_2 nanoparticles. In the next sections we resume and discuss different methods to obtain particles of uranium dioxide with grain sizes in the sub-micrometer range. We divided the methods by the type of synthesis. On one side, there are those which follow a wet chemical route, subdivided in processes that use a wet denitration step and processes which need an organic precursor, such as variation of sol-gel or Pechini syntheses. On the other side, we explain those methods which use irradiation with particles or photons to induce UO_2 particle formation. In addition, we describe biologically assisted syntheses, which make use of cells and bacteria to precipitate UO_2 nanoparticles.

It is worth to mention at this point that many of the published syntheses in articles or patents were focused to the production of UO_2 for its use in nuclear reactors. This application requires a powder with good fluency and compressibility to further handling for pellet fabrication. Thus, fractions of particles with sub-micrometer diameter, which sometimes are referred as “very fine powder,” were separated from the bulk and discarded. In addition, very often nanoparticles aggregate in micrometer-sized particles. Only with high-resolution microscopy techniques, or indirectly through BET surface area measurements, for example, it is possible to detect the nanometric structure of the material. Therefore, in more than one publication, nanoparticles are wrongly classified as micrometer-sized particles. Here we attract the attention on this fact in some of the reported works.

2. Chemical and electrochemical routes

2.1 Syntheses from inorganic uranyl salts

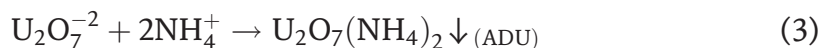
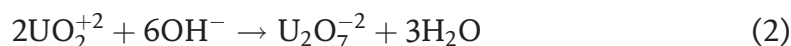
In the group of the wet chemical syntheses, one of the most common practices to obtain UO_2 to manufacture nuclear fuel pellets is the physicochemical precipitation, followed by calcination and reduction [12]. The ammonium di-uranate (ADU) and the ammonium uranyl carbonate (AUC) routes are two well-known examples. Both start from an inorganic uranium salt such as the uranyl nitrate hexahydrate (UNH), involve thermal treatments in different atmospheres and, at intermediate to high temperatures, obtain the fluorite fcc UO_2 phase.

Although the ADU synthesis originally was not tuned to produce nanoparticles, first studies describe that depending on pH and synthesis conditions, a fine powder with sub-micrometer structure and a grain size of 370 nm was observed [13]. Some years ago, Soldati et al. took advantage of characterization methods from the

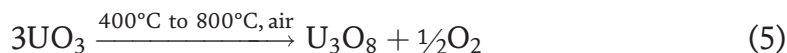
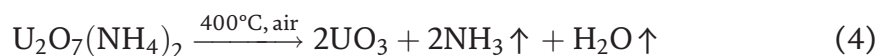
nanoscience and demonstrated that the UO_2 particles obtained by the ADU route in the standard conditions described elsewhere (i.e., pH 9 and 60°C thermal bath) were indeed agglomerates of rounded, but irregular, nanoparticles of homogeneous composition, fcc Fm-3 m crystal phase, and 80–120 nm crystal sizes [4]. In that experience, to obtain about 100 g UO_2 nanoparticles with those characteristics by the ADU method requires a filtrating step, produces about 2 L ammonia water waste, needs 12–16 hours thermal treatments at intermediate to high temperatures, and consumes air and a reducing atmosphere such as $\text{H}_2:\text{Ar}$ (10:90) [4, 13].

In these syntheses, UO_2 , and some mixed oxides with Gd or Pu, can be obtained from a solution of the actinides (as nitrates or oxides) in 1 M HNO_3 , concentrations of 50–400 g/L, 60°C, and pH between 4 and 9 [4, 13–16]. The precipitation of ADU is favored by mixing the mother solution with a basic 13 M (NH_4OH) solution [14, 15, 17] or bubbling NH_3 gas [4, 13] (Eqs. (1)–(3)).

For example, for the case of ADU, the involved reactions are:



Once that the precipitated phase is completely formed, the solution is stirred for 1 hour and vacuum filtrated, washed with milliQ water, and dried between 80 and 120°C for 24 hours. After that, the ADU is converted to U_3O_8 by calcination at 800°C in air for 6–8 hours (Eqs. (4) and (5)).



Finally, the U_3O_8 is reduced to UO_2 by thermal treatment between 650 and 700°C for 7 hours in pure H_2 or mixtures of H_2 and Ar or N_2 in proportions of 8–10% (Eq. (6)).



On the other side, the AUC, for example, is precipitated from the UNH- HNO_3 solution with $(\text{NH}_4)_2\text{CO}_3$ [14] and converted to UO_2 at 650°C in a water vapor/hydrogen atmosphere. However, to the best of our knowledge, only micrometric particle sizes were reported by AUC syntheses.

2.2 Syntheses from organic uranyl salts

An alternative way for precipitating UO_2 nanoparticles from the inorganic salt uranyl nitrate are the synthesis from the organic salts uranyl acetylacetonate (UAA) or acetate (UA), mediated by organic solvents and temperature. Wu et al., for example, obtained 3–8-nm-large cubic UO_2 nanocrystals by decomposition at 295°C, under Ar, of UAA in a mixture of oleic acid (OA), oleylamine (OAm), and octadecene (ODE) [18]. Non-agglomerated and highly crystalline UO_2 particles were obtained in a similar synthesis by Hudry et al. at temperatures of 280°C [19]. These nanoparticles were isotropic faceted nanodots of 3.6 ± 0.4 nm diameter. Moreover, Hu et al. used UA dissolved in oleylamine (OAm) and oleic acid (OA) which after heating in an oil bath, centrifuging, washing with ethanol, and

dispersing in cyclohexane resulted in two-dimensional nanoribbons of U_3O_8 with dimensions of about 4×100 nm. Higher autogenous pressure, in an autoclave, was useful for obtaining wider nanoribbons. With the addition of octadecene (ODE) or toluene, U_3O_7 nanowires were obtained whose width is about 1 nm and length varied in the range of 50–500 nm depending on the temperature-time conditions of the process [20]. In addition, sphere-shaped UO_2 nanoparticles with an average diameter of 100 nm, which consisted in 15 nm nanocrystal subunits, were obtained by Wang et al. from a 0.5 mM UA aqueous solution mixed with ethylenediamine, autoclaved, and heated at 160°C for 48 h [21]. On the other hand, Tyrpekl et al. obtained 5–11 nm UO_2 nanoparticles by annealing a dry precipitate of $(\text{N}_2\text{H}_5)_2\text{U}_2(\text{C}_2\text{O}_4)_5 \times n\text{H}_2\text{O}$ at 600°C in Ar [22].

2.3 Sol-gel syntheses

A colloid is a suspension in which the dispersed phase particle's size is so small (~ 1 –1000 nm) that gravitational forces are negligible and interactions are dominated by short-range forces, such as van der Waals attraction and surface charges. In the context of the sol-gel synthesis, the “sol” is formed by a colloidal suspension of solid particles in a liquid, while the “gel” is a suspension of a liquid phase in a continuous solid phase [23]. Basically, two sol-gel routes are used: the polymeric route using alkoxides and the colloidal route using metal salts.

In a typical polymeric sol-gel process, as the one used for low-temperature preparation of SiO_2 monoliths from a tetraethoxysilane (TEOS) solution, a polymerized structure is formed by the condensation of alcohols proceeding from the TEOS hydrolysis. Another widely used sol-gel synthesis is the complexation by amines, known as internal gelation [24–27]. This synthesis is common to find in the nuclear field associated to the fabrication of UO_2 microspheres formed by agglomerated nanoparticles as in the work of Daniels et al. [25]. In this case, an uranyl nitrate solution is mixed with urea ($\text{CO}(\text{NH}_2)_2$) and hexamethylenetetramine (HMTA) solution. Then, the HMTA is decomposed at low temperature (90°C) causing an increase in pH and hydrolysis of uranium (Eqs. (7) and (8)), resulting in a solution gelation:



This gel is washed with NH_4OH and dried to obtain dry UO_3 . Later, thermal treatments at 800°C in air allow obtaining U_3O_8 powders that are further reduced to UO_2 particles. With this method, UO_2 millimeter-sized spheres with a nanometric substructure were obtained by different authors [25, 26]. The powder morphologies and particle sizes depend on the temperature and the calcination atmospheres used. The average particle size varies between 100 and 4000 nm. The samples obtained through the oxalic route and a single calcination (in neutral or reductive atmosphere) showed similar lattice parameters, close to the value of UO_2 [24].

Recently Leblanc et al. presented another method that they called “advanced thermal denitration in presence of organic additives” that includes a gelation step of the uranyl nitrate solution [28]. In this process, an acidic uranyl nitrate solution is prepared, and urea is added to avoid uranium precipitation. Oxide synthesis was performed by adding two monomer types: acrylic acid (AA) and N,N'-methylene bis acrylamide (MBAM) in a molar ratio of 20:1 (AA:MBAM). A fully homogeneous solution was obtained, which when heated up to 100°C and after the addition of 25 mL of hydrogen peroxide (30 wt%) as initiator completely polymerized into a

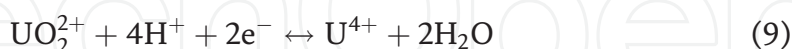
gel. The entire solution is incorporated into the polymer network, ensuring that all the cations of the system are stripped into the obtained gel. Drying at 150°C, following an oxidative calcination of the organic part at 800°C, and finally reducing it in Ar:5%H₂ at 800°C resulted in a nanostructured material with crystallite size below 100 nm, as determined by XRD diffraction.

2.4 Electrochemically assisted syntheses

Recently, Rousseau et al. presented a wet chemical novel method to synthesize UO₂ (and also UO₂ doped with tetra- or trivalent elements), based on the electrochemical reduction of U⁶⁺ to U⁴⁺, followed by a precipitation in a reducing and anoxic condition, at constant pH [29]. The mother U⁴⁺ solution was made dissolving UNH in 1 M NaCl. The authors studied two methods for precipitating stable UO_{2+x} nanoparticles of different sizes. In the pH range 2.5–4, the starting U⁶⁺ solution was added to the NaCl solution under reducing conditions, and U⁶⁺ cations were reduced electrochemically to U⁴⁺. The increment in pH was compensated with 0.1 M HCl. In the pH range 4–8, the mother U⁶⁺ solution was added drop by drop directly to the 1 M NaCl solution, balancing the pH change with 0.1 M NaOH. A redox potential of –300 mV/NHE was applied using Pt electrodes. The obtained products were filtered with a 0.22 µm filter, and the precipitates were washed two times with ultrapure water. The nanoparticles produced correspond to a single fluorite UO_{2.19 ± 0.01} phase and average TEM coherent domain size of (12 ± 2) nm for pH < 4 and UO_{2.11 ± 0.02} of 4–6 nm for pH 6.5. The BET surface area for this nanomaterial was 10.3 ± 0.1 m²/g, which the authors associated to a grain size of 53 nm, indicating a moderate agglomeration of the nanoparticles. XPS, in good agreement with the other analytical techniques, resulted in a U⁶⁺/U⁴⁺ ratio close to 0.1.

Moreover, an electrolytically reduced aqueous solution of 0.5 M uranyl nitrate was used as precursor, together with NaOH solution as alkalinization agent, to trigger the precipitation of UO₂ nanoparticles near the U⁴⁺ solubility line. XRD and HR-TEM analyses showed that the nanoparticles obtained exhibit the typical slightly oxidized UO_{2+x} fcc fluorite structure, with an average crystal size of 3.9 nm and a narrow size distribution [6].

In these cases, the reduction is mediated by the reactions occurring in the cathode (Eq. (9)) and in the anode (Eq. (10)), respectively [6]:



To maintain the reducing environment, the oxygen must be eliminated with an oxygen-free gas such as pure Ar. In the work of Jovani-Abril et al. [6], for example, the starting pH was 0.5, and the solution was slowly alkalinized to allow the precipitation of the UO₂ nanoparticles, following the equation:



2.5 Fluidized bed syntheses

Thermal denitration in a fluidized bed is another way to indirectly obtain UO₂ micro (and nano) particles. It involves spraying a concentrated solution of UNH on a bed of UO₃ at moderated temperatures (240–450°C) and fluidizing it with air or steam. The UO₃ produced nucleates on the existing UO₃ particles of the bed,

enlarging their volume, or forming new particles. Afterward, thermal treatments can be used to convert the UO_3 to U_3O_8 and UO_2 . This method uses less chemicals than the precipitation type of syntheses and allows the recuperation of the solvents but reported grain sizes are in the 100–500 μm [30], i.e., three orders of magnitude larger than the nanoparticles. However, it should be noted here that the equipment reviewed in most of the publications regarding fluidized beds are tuned to fabricate nuclear fuels. Under certain conditions of bed lengths, temperature, and solution feed speed, the authors reported the formation of “a very fine powder, not well suited to the subsequent powder handling” that is elutriated in the process [31]. This means that those grains smaller than some microns were separated by their different density, grain size and morphology in the vapor/gas stream, losing all information about the possible existence of nanoparticles. Thus, it is possible that nanoparticles would be obtained in fluidized bed denitration by tuning appropriate operative characteristic.

3. Radiation-assisted syntheses

This type of UO_2 nanoparticles syntheses focus on the reduction of U^{6+} to U^{4+} by some kind of radiation. The process is induced exposing an aqueous solution of U^{6+} and an organic precursor to beta particles or photons including gamma and X-rays.

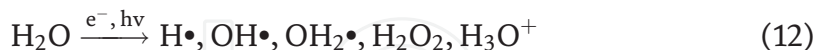
When particles are used, they are typically 4.5–7 MeV electrons from particle accelerators [32–35]. For example, Roth et al. used a pulsed beam with a frequency of 12.5 Hz and 4 μs pulse duration with an average dose rate of 24 Gy/s. To get a dose of 15 kGy, 625 s of effective irradiation must be accumulated. Conversion efficiency of U^{6+} to U^{4+} was 95% after 15 kGy delivered dose. However, Pavelková et al. used doses up to 100 kGy of 4.5 MeV electrons. In the first case, the authors obtained a narrow size distribution of 22–35 nm nanoparticles and a BET surface area of 60–70 m^2/g [35]. In the second case, heat treatments were necessary to obtain well-developed nanocrystals with linear crystallite size 13–27 nm and specific surface area 10–46 m^2/g [32].

On the other hand, gamma-ray photons consist mainly in those from ^{60}Co radiation sources (two emissions of 1.17 and 1.33 MeV). Dose rates in the order of 198 Gy/h are delivered, and after 70 h of irradiation, 65% of conversion efficiency was obtained in the work of Roth et al. [35]. Nenoff et al. used also a 198 Gy/h setup, but irradiation times from 7 to 10 days. In these conditions, nanoparticles readily form in the solution [36]. After 7 days of irradiation time, Roth et al. obtained nanoparticles of around 80 nm [35], and Nenoff et al. found in fresh prepared solution 6 nm particles, while aging resulted in their agglomeration. In that work, the crystal phase was studied from the TEM diffraction pattern resulting in alpha (α)-U or orthorhombic U metal phase (space group Cmcm). These particles converted naturally to the fcc UO_2 crystal phase, when allowed to rest in air by some days [36].

Moreover, X-rays can be used also to generate nanoparticle precursors in the bulk of an uranyl nitrate solution, which after a thermal treatment below 600°C, transform to UO_2 nanoparticles. X-rays from medium pressure 140 W mercury lamps have been used for this purpose [32, 37, 38]. In medium-pressure mercury-vapor lamps, the lines from 200 to 600 nm are present, namely 253.7, 365.4, 404.7, 435.8, 546.1, and 578.2 nm. However in this case, the 253.7 nm line is the one of interest. Illumination times between 60 and 180 minutes were used to obtain the nanoparticle precursors. After that, a heat treatment under Ar:H_2 atmosphere at 550°C was done in order to form the UO_2 nanoparticles. A yield of 70% was obtained with this method. Nanoparticles obtained were monocrystals of 14.9 nm as determined by XRD spectra in accordance with TEM images and presented a specific surface area of 10.4 m^2/g .

3.1 Precursor formation: U^{6+} to U^{4+} reduction and polymerization

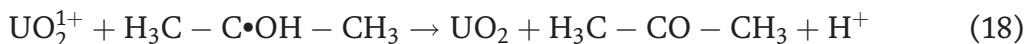
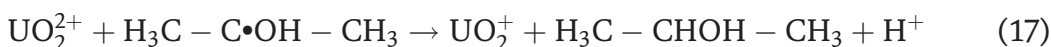
Regardless of the type of radiation used, U^{6+} is in the form of an uranyl nitrate $UO_2(NO_3)_2$ acidic aqueous solution and the uranyl concentrations used range from 10 to 50 mM. The chemical reduction reactions, which were presented by Rath et al., are described next [34]. The irradiation with electrons or photons produces water photolysis:



where $H\bullet$ is a reducing agent and $OH\bullet$ is an oxidizing radical. By adding an organic species, which commonly is a secondary alcohol, these species are scavenged, and a strongly reducing agent is produced (reactions Eqs. (14) and (15)). Propan-2-ol, for example, reacts with both $H\bullet$ and $OH\bullet$ forming a strongly reducing 1-hydroxy 2-propyl radical $H_3C-C\bullet OH CH_3$:



Thus, in that milieu, the following reducing and polymerization reactions are possible:



The following reaction (Eq. (20)) is also possible, which retires hydrated electrons from the solution, though NO_3^{-2} anions finally convert to NO_3^- :



During irradiation, there is UO_2^{2+} consumption to form the UO_2° nanoparticles. The UV-visible absorption spectra of uranyl nitrate exhibit maxima at 427, 477, and 495 nm; the maxima gradually disappear during irradiation, due to the precipitation of the precursor. This is a usual way to follow the nanoparticle precursor formation kinetics during irradiation.

According to Rath et al., an induction time of 135 min after irradiation was necessary for the nanoparticles to form in the presence of 1% volume fraction of propan-2-ol and 50 kGy of absorbed dose [34]. The same work shows that this value depends on the scavenger concentration and the viscosity of the uranyl solution. Induction time also increased with the ethylene glycol concentration, which was used to obtain higher viscosity values.

4. Biologically assisted synthesis

Nanoparticles UO_2 can be obtained also by mediation of living organisms. *Shewanella* genus, for example, belongs to a well-known group of U^{6+} reducing bacteria. Within this group, anaerobic *Shewanella oneidensis* MR-1 and *Shewanella*

putrefaciens CN32 species have been widely used by several authors to produce biogenic uraninite nanoparticles [39–42]. Other species studied were: *Desulfovibrio vulgaris* [43, 44], *Geobacter sulfurreducens* [45, 46], and *Anaeromyxobacter dehalogenans* 2CP-C [47].

One of the main interests related to this topic is the possible use of bacteria in reducing the environmental mobility of the U^{6+} ions by transforming them into U^{4+} species. Thus, there is a big effort in determining the factors that affect the physiological state of the microorganisms, which mediate the U^{6+} reduction, as well as in determining which geochemical and environmental conditions modify the nanobiogenic UO_2 surface reactivity [40] and redox potentials [42].

These experiments are conducted in a series of stages: the preparation of a background electrolyte, where the bacteria is allowed to live and growth, the cell cultivation, the U^{6+} bioreduction experiments and, finally, the determination of U^{4+} re-oxidation rates under different conditions. In natural environments, uranium might be present in different sites due to the geology of the area but also as a contaminant in soils, sediments, and groundwater [40]. So, on the one hand, the background electrolyte implies the preparation of buffered (6.8–8 pH range) artificial groundwater made of uranyl acetate in 1.2–4 mM concentrations and some organic additives as lactic acid and macronutrients for bacterial growth. On the other hand, cell suspensions are cultured aerobically at 30°C for 24 h; centrifuged, washed with an anaerobic buffer, and resuspended in an anaerobic solution. From this suspension, a portion is inoculated into the buffered, anaerobic uranyl-bearing solution to initiate uranium reduction. After a bioreduction essays, cell-uranium precipitates are pasteurized at 70°C to deactivate biological activity [40–42]. Burgos et al., for example, reported that it was challenging to determine what constitutes a single discrete particle in samples with thick uraninite coatings or large extracellular deposits but regardless of the bioreduction rate or the electrolyte used, identified a mean particle size structure of around 3 nm in TEM micrographs as well as with X-ray absorption fine structure spectroscopy (EXAFS) [39], while Singer et al. found stoichiometric uraninite with particle diameters of 5–10 nm by DRX [40].

Probably one of the most interesting results obtained by these authors was that the bioreduction rate is not the unique factor which controls the particle size of biogenic uraninite. Within the parameters that influence the obtaining of certain particle size, it can be include cell cultivation methods, metabolic state of cells, molecular-scale mechanisms of U^{6+} reduction, U^{4+} nucleation site, and cellular location of uraninite precipitates [39].

5. Conclusions

With the recent knowledge gained on nanoscience and nanomaterials, and the complex interaction that nanoparticles have in the environment, there is a new insight toward nanoparticles generated from the nuclear technology. It is a fact that long-term nuclear waste disposals and nuclear reactors are sources of UO_2 and actinide- and lanthanide-doped UO_2 nanoparticles. Therefore there is an effort to produce nanoparticles of these compositions to study not only their behavior in special physicochemical conditions but also their advantageous properties in the design of new fuel elements and processes.

There exist many ways to obtain nanoparticles of UO_2 , but until now all of them start from a solution of U^{6+} and reduces it to U^{4+} . The way in which the nanoparticle is formed or the reduction is done differentiates one of the other processes. In the precipitation routes, the pH generates nanoparticles of U^{6+} salts that after intermediate- to high-temperature thermal treatments in reducing conditions convert to

micrometer agglomerates of UO_2 nanoparticles of 80–120 nm and fcc crystal phase. Other chemical routes use U^{6+} organic salts in an organic solvent as dibenzyl ether, with amines and organic acids as stabilization agents, to induce the precipitation of non-agglomerated and highly crystalline UO_2 nanoparticles of less than 5 nm during a low-temperature thermal treatment. In the sol-gel type syntheses, nanoparticles with U^{6+} are generated in the continuous solid phase, sometimes mediated by the addition of organic molecules. The gel is dried after and reduced to obtain micrometer-sized agglomerates of UO_2 nanoparticles of around 90 nm crystallite size. In the electrochemical-assisted syntheses, electrons are directly supplied at the cathode to the uranyl solution to reduce the uranium ions to U^{4+} , which precipitates as moderately agglomerated powders of 53 nm formed by 4–14 nm crystal size UO_2 nanoparticles. The processes assisted by radiation consist in generating strongly reducing organic agents by irradiating a secondary alcohol with electrons or photons. These species reduce the U^{6+} to U^{4+} in the solution forming UO_2 , which aggregates in crystalline nanoparticles. In case of electron irradiation, small particles with a narrow size distribution (22–35 nm) were obtained, while for gamma irradiation 3.5–5 nm particles were formed. In case of X-rays photons, the product obtained are precursors of nanoparticles and need a subsequent intermediate-temperature thermal treatment to definitely form the UO_2 nanoparticles with 3–15 nm and fcc crystal phase.

Acknowledgements

The authors thank the INN for the financial support to publish this chapter.

Author details


Analía Leticia Soldati^{1,2*}, Diana Carolina Lago¹ and Miguel Oscar Prado^{1,2}

1 Nuclear Materials Department, Bariloche Atomic Center, National Atomic Energy Commission (CNEA), San Carlos de Bariloche, Argentina

2 Institute of Nanoscience and Nanotechnology (INN), National Commission of Science and Technology Research (CONICET), San Carlos de Bariloche, Argentina

*Address all correspondence to: asoldati@cab.cnea.gov.ar

IntechOpen

© 2020 The Author(s). Licensee IntechOpen. This chapter is distributed under the terms of the Creative Commons Attribution License (<http://creativecommons.org/licenses/by/3.0>), which permits unrestricted use, distribution, and reproduction in any medium, provided the original work is properly cited. 

References

- [1] Hochella MF et al. Natural, incidental, and engineered nanomaterials and their impacts on the Earth system. *Science*. 2019;**363**(6434): eaau8299
- [2] Spino J, Vennix K, Coquerelle M. Detailed characterisation of the rim microstructure in PWR fuels in the burn-up range 40-67 GWd/tM. *Journal of Nuclear Materials*. 1996;**231**(3): 179-190
- [3] Spino J et al. Bulk-nanocrystalline oxide nuclear fuels—An innovative material option for increasing fission gas retention, plasticity and radiation-tolerance. *Journal of Nuclear Materials*. 2012;**422**(1–3):27-44
- [4] Soldati AL et al. Synthesis and characterization of Gd₂O₃ doped UO₂ nanoparticles. *Journal of Nuclear Materials*. 2016;**479**:436-446
- [5] Cappia F et al. Laser melting of nano-crystalline uranium dioxide. *Progress in Nuclear Energy*. 2014;**72**(0):11-16
- [6] Jovani-Abril R et al. Synthesis of nc-UO₂ by controlled precipitation in aqueous phase. *Journal of Nuclear Materials*. 2016;**477**:298-304
- [7] Nenoff TM et al. Synthesis and low temperature in situ sintering of uranium oxide nanoparticles. *Chemistry of Materials*. 2011;**23**(23):5185-5190
- [8] Kalmykov SN, Denecke M. *Actinide Nanoparticle Research*. Berlin Heidelberg: Springer-Verlag; 2011
- [9] Neill TS et al. Silicate stabilisation of colloidal UO₂ produced by uranium metal corrosion. *Journal of Nuclear Materials*. 2019;**526**:151751
- [10] Fuller EL et al. Uranium oxidation: Characterization of oxides formed by reaction with water by infrared and sorption analyses. *Journal of Nuclear Materials*. 1984;**120**(2):174-194
- [11] Kaminski MD et al. Colloids from the aqueous corrosion of uranium nuclear fuel. *Journal of Nuclear Materials*. 2005;**347**(1):77-87
- [12] Weber WG et al. Chapter 2: Preparation of uranium dioxide. In: Belle J, editor. *Uranium Dioxide: Properties and Nuclear Applications*. Washington: Naval Reactors, Division of Reactor Development USA Energy Commission; 1921. pp. 35-64
- [13] Menghini J et al. Mixed oxide pellets obtention by the "Reverse Strike" co-precipitation method. Session 1: Optimization of fuel fabrication technology practices and modelling. In: Bibilashvili Y, Dörr W, editors. *IAEA Technical Meeting*. Brussel, Belgien: IAEA; 2004. pp. 31-44
- [14] Riella HG et al. UO₂-Gd₂O₃ solid solution formation from wet and dry processes. *Journal of Nuclear Materials*. 1991;**178**(2–3):204-211
- [15] Fukushima S et al. The effect of gadolinium content on the thermal conductivity of near-stoichiometric (U, Gd)O₂ solid solutions. *Journal of Nuclear Materials*. 1982;**105**(2):201-210
- [16] Miyake C, Kanamaru M, Imoto S. Microcharacterization of gadolinium in U_{1-x}Gd_xO₂ by means of electron spin resonance. *Journal of Nuclear Materials*. 1986;**137**(3):256-260
- [17] Durazzo M et al. Phase studies in the UO₂-Gd₂O₃ system. *Journal of Nuclear Materials*. 2010;**400**(3):183-188
- [18] Wu H, Yang Y, Cao YC. Synthesis of colloidal uranium-dioxide nanocrystals. *Journal of the American Chemical Society*. 2006;**128**(51):16522-16523

- [19] Hudry D et al. Non-aqueous synthesis of isotropic and anisotropic actinide oxide nanocrystals. *Chemistry—A European Journal*. 2012; **18**:8283-8287
- [20] Hu S et al. Nanocrystals of uranium oxide: Controlled synthesis and enhanced electrochemical performance of hydrogen evolution by Ce doping. *Small*. 2015; **11**(22):2624-2630
- [21] Wang Q et al. Synthesis of uranium oxide nanoparticles and their catalytic performance for benyl alcohol conversion to benzaldehyde. *Journal of Materials Chemistry*. 2008; **18**:1146-1152
- [22] Tyrpekl V et al. Low temperature decomposition of U(IV) and Th(IV) oxalates to nanograined oxide powders. *Journal of Nuclear Materials*. 2015; **460**: 200-208
- [23] Brinker CJ, Scherer GW. Chapter 1—Introduction. In: Brinker CJ, Scherer GW, editors. *Sol-Gel Science*. San Diego: Academic Press; 1990. pp. xvi-18
- [24] Ziouane Y et al. Effect of the microstructural morphology on UO_2 powders. *Procedia Chemistry*. 2016; **21**: 319-325
- [25] Daniels H et al. Fabrication of oxidic uranium-neodymium microspheres by internal gelation. *Progress in Nuclear Energy*. 2012; **57**:106-110
- [26] Schreinemachers C et al. Characterization of uranium neodymium oxide microspheres synthesized by internal gelation. *Progress in Nuclear Energy*. 2014; **72**: 17-21
- [27] Gündüz G, Önal I, Durmazuçar HH. Pore size distributions in uranium dioxide and uranium dioxide-gadolinium oxide fuel kernel produced by sol-gel technique. *Journal of Nuclear Materials*. 1991; **178**(2-3):212-216
- [28] Leblanc M et al. Actinide mixed oxide conversion by advanced thermal denitration route. *Journal of Nuclear Materials*. 2019; **519**:157-165
- [29] Rousseau G et al. Synthesis and characterization of nanometric powders of UO_{2+x} , $(\text{Th}, \text{U})\text{O}_{2+x}$ and $(\text{La}, \text{U})\text{O}_{2+x}$. *Journal of Solid State Chemistry*. 2009; **182**(10):2591-2597
- [30] Fane A, Charlton B, Alfredson P. *The Thermal Denitration of Uranyl Nitrate in a Fluidised Bed Reactor*. Sidney: ANSTO; 1974
- [31] Harrington CD, Ruehle AE. *Uranium Production Technology*. Princeton, New Jersey: D. Van Nostrand Company Inc.; 1959
- [32] Pavelková T et al. E-beam and UV induced fabrication of CeO_2 , Eu_2O_3 and their mixed oxides with UO_2 . *Radiation Physics and Chemistry*. 2016; **124**: 252-257
- [33] Rath MC, Naik DB. Post-irradiation induction time in the radiolytic synthesis of UO_2 nanoparticles in aqueous solutions. *Journal of Nuclear Materials*. 2014; **454**(1):54-59
- [34] Rath MC, Naik DB, Sarkar SK. Reversible growth of UO_2 nanoparticles in aqueous solutions through 7.0 MeV electron beam irradiation. *Journal of Nuclear Materials*. 2013; **438**(1-3):26-31
- [35] Roth O, Hasselberg H, Jonsson M. Radiation chemical synthesis and characterization of UO_2 nanoparticles. *Journal of Nuclear Materials*. 2009; **383**(3):231-236
- [36] Nenoff TM et al. Formation of uranium based nanoparticles via gamma-irradiation. *Journal of Nuclear Materials*. 2013; **442**(1-3):162-167
- [37] Pavelková T et al. Preparation of UO_2 , ThO_2 and $(\text{Th}, \text{U})\text{O}_2$ pellets

from photochemically-prepared nano-powders. *Journal of Nuclear Materials*. 2016;**469**:57-61

[38] Pavelková T, Čuba V, Šebesta F. Photo-induced low temperature synthesis of nanocrystalline UO_2 , ThO_2 and mixed UO_2 - ThO_2 oxides. *Journal of Nuclear Materials*. 2013;**442**(1):29-32

[39] Burgos WD et al. Characterization of uraninite nanoparticles produced by *Shewanella oneidensis* MR-1. *Geochimica et Cosmochimica Acta*. 2008;**72**(20): 4901-4915

[40] Singer DM, Farges F, Brown GE Jr. Biogenic nanoparticulate UO_2 : Synthesis, characterization, and factors affecting surface reactivity. *Geochimica et Cosmochimica Acta*. 2009;**73**(12): 3593-3611

[41] Schofield EJ et al. Structure of biogenic uraninite produced by *Shewanella oneidensis* strain MR-1. *Environmental Science & Technology*. 2008;**42**(21):7898-7904

[42] Ulrich K-U et al. Comparative dissolution kinetics of biogenic and chemogenic uraninite under oxidizing conditions in the presence of carbonate. *Geochimica et Cosmochimica Acta*. 2009;**73**(20):6065-6083

[43] Zhou C et al. Growth of *Desulfovibrio vulgaris* when respiring U(VI) and characterization of biogenic uraninite. *Environmental Science & Technology*. 2014;**48**(12):6928-6937

[44] Lovley DR et al. Reduction of uranium by cytochrome c3 of *Desulfovibrio vulgaris*. *Applied and Environmental Microbiology*. 1993; **59**(11):3572-3576

[45] Sharp JO et al. Uranyl reduction by *Geobacter sulfurreducens* in the presence or absence of iron. In: Merkel BJ, Hasche-Berger A, editors. *Uranium,*

Mining and Hydrogeology. Berlin, Heidelberg: Springer; 2008

[46] Bargar JR, et al. Coupled biogeochemical processes governing the stability of bacteriogenic UO_{2+x} . In: 3rd Annual DOE-ERSP PI Meeting. Lansdowne, Virginia; 2008

[47] Wu Q, Sanford RA, Löffler FE. Uranium(VI) reduction by *Anaeromyxobacter dehalogenans* strain 2CP-C. *Applied and Environmental Microbiology*. 2006;**72**(5):3608-3614